

Mechanism-Based Probe for the Analysis of Cathepsin Cysteine Proteases in Living Cells

Howard C. Hang^{†,*}, Joana Loureiro[†], Eric Spooner[†], Adrianus W. M. van der Velden[§], You-Me Kim[†], Annette M. Pollington[†], Rene Maehr[¶], Michael N. Starnbach[§], and Hidde L. Ploegh^{†,*}

[†]Whitehead Institute for Biomedical Research, Massachusetts Institute of Technology, Cambridge, Massachusetts 02142,

[§]Department of Microbiology and Molecular Genetics, Harvard Medical School, Boston, Massachusetts 02115, ^{*}Current address: Laboratory of Chemical Biology and Microbial Pathogenesis, The Rockefeller University, New York, New York 10021, [¶]Current address: Department of Molecular Cell Biology, Harvard University, Cambridge, Massachusetts 02142

The explosion of genomic sequences from many organisms has provided unprecedented opportunities for the global analysis of complex biological processes. While the advances in nucleotide microarrays and mass spectrometry (MS) have enabled large-scale comparative analyses of gene and protein expression, respectively, these technologies do not fully reveal the functional complexity of proteomes that are regulated by post-transcriptional/translational mechanisms. To address the functional complexity of proteomes, new chemical strategies have been developed for the targeted analysis of individual protein superfamilies (1). In particular, mechanism-based probes have been developed for covalent labeling of enzyme families through active site nucleophiles (*i.e.*, serine hydrolases (2) and cysteine proteases (3–5)) or by photochemical cross-linking (metalloproteases) (6, 7). These mechanism-based probes are typically appended with chemical or epitope tags such as ¹²⁵I, fluorophores, or biotin to visualize covalently labeled polypeptides in cell lysates or tissue samples after gel-based separation. Since these mechanism-based probes are designed to target the active site of enzymes, the extent of protein labeling with these chemical probes often reflects the amount of active enzyme present in the sample, which provides details of function not available by measuring transcript or protein abundance alone. These chemical approaches have been termed activity-based protein profiling and have provided insight into protein function previously unattainable by either gene or protein expression analyses (1). Mechanism-based probes are also providing new tools for drug discovery, small-molecule target identification, and the discovery of previously uncharacterized protein activities (1).

ABSTRACT Mechanism-based probes are providing new tools to evaluate the enzymatic activities of protein families in complex mixtures and to assign protein function. The application of these chemical probes for the visualization of protein labeling in cells and proteomic analysis is still challenging. As a consequence, imaging and proteomic analysis often require different sets of chemical probes. Here we describe a mechanism-based probe, azido-E-64, that can be used for both imaging and proteomics. Azido-E-64 covalently modifies active Cathepsin (Cat) B in living cells, an abundant cysteine protease involved in microbial infections, apoptosis, and cancer. Furthermore, azido-E-64 contains an azide chemical handle that can be selectively derivatized with phosphine reagents *via* the Staudinger ligation, which enables the imaging and proteomic analysis of Cat B. We have utilized azido-E-64 to visualize active Cat B during infection of primary macrophages with *Salmonella typhimurium*, a facultative intracellular bacterial pathogen. These studies demonstrated that active Cat B is specifically excluded from *Salmonella*-containing vacuoles, which suggests that inhibition of protease activity within bacteria-containing vacuoles may contribute to bacterial virulence.

*Corresponding authors,
ploegh@wi.mit.edu, hang@wi.mit.edu.

Received for review October 18, 2006
and accepted November 15, 2006.

Published online December 8, 2006

10.1021/cb600431a CCC: \$33.50

© 2006 by American Chemical Society

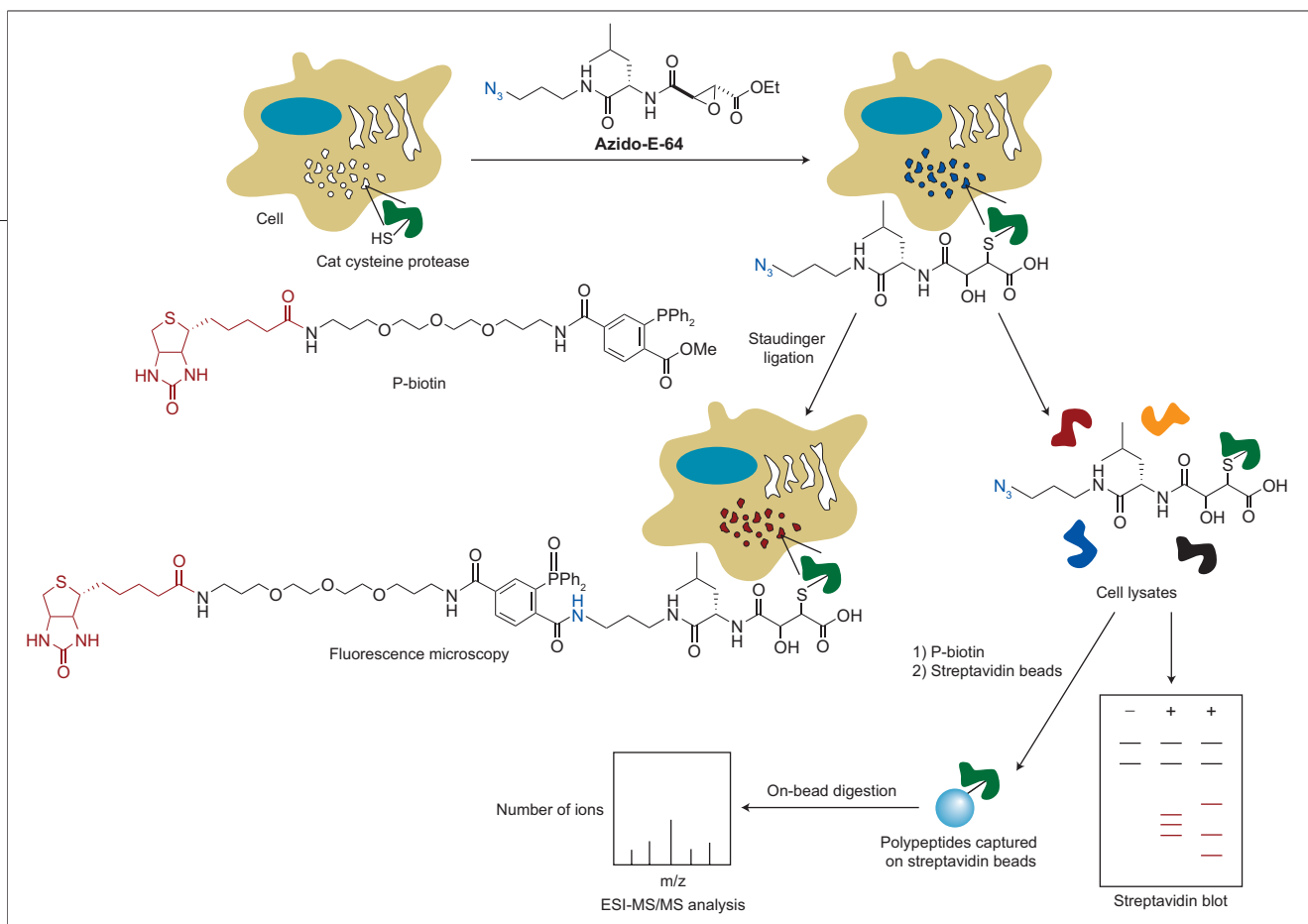


Figure 1. Mechanism-based probe for labeling active Cat cysteine proteases in living cells. Treatment of cells with azido-E-64 enables covalent modification of Cat cysteine proteases in living cells. Reaction of the azide chemical handle on azido-E-64 with p-biotin via the Staudinger ligation allows visualization of active proteases by fluorescence microscopy or streptavidin blot and also enables proteomic analysis of azido-E-64-labeled proteins by MS after affinity enrichment with streptavidin beads.

Microbial pathogens utilize complex mechanisms to infect host cells and cause disease, which requires new approaches to dissect these interactions for therapeutic intervention (8). Mechanism-based probes present novel chemical tools to understand microbial pathogenesis. For example, the application of mechanism-based probes to the *Plasmodium falciparum* life cycle suggested the cysteine protease falcipain 1 plays an essential role during parasite invasion of host cells and may be a target for antimalarial therapeutics (9). We recently used a mechanism-based probe for deubiquitinating enzymes to assess the role of these cysteine proteases during herpesvirus infection (3, 10). Our analysis uncovered a new family of virally encoded deubiquitinating enzymes embedded within the tegument protein that is conserved throughout the herpesviridae (11), the deubiquitinating activities of which were not evident from bioinformatic analysis of viral genomes. Furthermore, this mechanism-based probe has identified deubiquitinating enzymes from *Chlamydia trachomatis*, a Gram-negative bacterial pathogen with currently no available methods for genetic manipulation (12) as well as the parasite *P. falciparum* (13). Chemical probes are beginning to provide new insights into microbial pathogen-

esis; however, cell-permeable mechanism-based probes will be required to understand these complex interactions *in vivo*.

While mechanism-based probes have enabled the selective profiling of various enzyme families in complex mixtures *in vitro* (1), significant challenges still exist for the application of these mechanism-based probes to living cells and for proteomic analysis of labeled proteins. Large chemical tags, such as biotin or fluorophores utilized for the visualization or proteomic analysis of labeled polypeptides, may alter the specificity of protein labeling or passive diffusion into cells. These challenges have necessitated different sets of probes for proteomic analysis and for imaging. For example, the epoxysuccinate mechanism-based probe DCG-04 provides an excellent tool for the proteomic analysis of the Cathepsin (Cat) cysteine protease family (4, 14). However, the biotin moiety on DCG-04 prevents passive diffusion of this probe across cellular membranes, which precludes its application to living cells (4, 14). Fluorophore-modified derivatives of DCG-04 have also been generated for visualization of Cat cysteine proteases in live cells (15) and *in vivo* (16), but these have limitations due to background fluorescence of unbound

probes. Recently, the development of quenched activity-based probes (qABPs) by Blum *et al.* (17) provides an elegant method to visualize Cat cysteine proteases in cells. These qABPs are based on acyloxyl methyl ketone mechanism-based probes that are modified with a fluorophore and quencher. The latter departs following protein labeling to yield a fluorescently tagged enzyme (17). Collectively, biotinylated probes (4) and qABPs (17) afford two different sets of ABPs for proteomics and imaging, respectively. Ideally, a single ABP could function for both proteomic analysis and imaging in cells.

The development of two bioorthogonal labeling reactions, the Staudinger ligation (18) and the Huisgen [3 + 2] cycloaddition (19), decouples protein labeling from visualization and proteomic analysis, which provides exciting opportunities for the application of mechanism-based probes in living cells and *in vivo*. The Staudinger ligation allows the use of the azide as a small chemical tag that can be converted into a variety of functionalities, including biotin or fluorophores by reaction with appropriately designed phosphine reagents (Figure 1) (18). Likewise, the Huisgen [3 + 2] cycloaddition, or “click-chemistry”, allows the azide or alkynes to be used as small chemical tags for subsequent attachment of visualization or affinity tags (20). In fact, these two-step labeling approaches have been applied toward mechanism-based probes for the in-cell labeling of the proteasome (21) and serine hydrolases (20), using the Staudinger ligation and click chemistry, respectively. More recently, these bioorthogonal reactions have enabled the MS-based proteomic analysis of azide- (22) and alkyne-labeled proteins (23, 24).

Here we describe a single-mechanism-based probe, azido-E-64, that enables live cell labeling of Cat cysteine proteases and subsequent proteomic analysis as well as visualization of Cat cysteine proteases in cells by fluorescence microscopy (Figure 1). Azido-E-64 is equipped with a small azide chemical handle that enables diffusion of the probe through cellular membranes. Proteomic analysis and visualization of the covalently modified proteases are accomplished after bioorthogonal labeling with a phosphine reagent *via* the Staudinger ligation (18) (Figure 1). Using this novel mechanism-based probe, we demonstrate active Cat B is excluded from *Salmonella*-containing vacuoles (SCVs) in primary macrophages, suggesting that inhibition of endocytic protease activity may contribute to the survival of intracellular bacterial pathogens.

RESULTS AND DISCUSSION

Azido-E-64 Irreversibly Labels Active Cat Cysteine

Proteases in Living Cells. To monitor the activity of the Cat cysteine proteases in living cells, we synthesized a mechanism-based probe azido-E-64 (Figure 2), along with a free acid derivative azido-E-64-OH (Figure 2 and Supplementary Figure 1). The design of these mechanism-based probes was based on the natural product E-64 (25) and DCG-04 (4) (Figure 2, panel a), two well-characterized epoxysuccinate protease inhibitors that covalently modify the active site thiol of Cat cysteine proteases. The inhibitory activity of azido-E-64 and azido-E-64-OH was evaluated by incubation of cell lysates from the RAW264.7 macrophage cell line with increasing concentrations of the mechanism-based probes and assayed for DCG-04 labeling to visualize the remaining active sites not already modified (Figure 2, panel b). E-64 was also included in these assays for comparison (Figure 2). DCG-04 covalently modifies the active site thiol of Cat cysteine proteases, which is then detected by virtue of the biotin moiety in DCG-04 after SDS-PAGE followed by streptavidin–horseradish peroxidase (HRP) blotting (4, 14). Azido-E-64 was less potent at blocking DCG-04 labeling *in vitro* compared to E-64 or azido-E-64-OH (Figure 2, panel b). In contrast, preincubation of live macrophages with azido-E-64 abrogated DCG-04 labeling of cell lysates more efficiently than did E-64 or azido-E-64-OH and completely blocked labeling with DCG-04 at 13 μ M azido-E-64 (Figure 2, panel c). The greater potency of azido-E-64 compared to E-64 or azido-E-64-OH in cells is presumably due to the ethyl ester on azido-E-64, which is likely converted into the free acid by nonspecific esterases within cells. These observations are consistent with previous reports comparing E-64 derivatives (26).

To visualize cellular targets of azido-E-64 directly, cell lysates from macrophages treated with azido-E-64 were reacted with phosphine-biotin (p-biotin) for bioorthogonal labeling of azide-modified proteins (Figure 1). In the absence of azido-E-64, no p-biotin labeling was observed in the molecular mass range (20–37 kDa) expected for the Cat cysteine proteases (Figure 3). The intensity of azido-E-64 labeling increased in a dose-dependent manner (Figure 3, panel a). Azido-E-64 labeling was also time-dependent, was observable within 5 min of incubation, and reached saturation within 40 min (Figure 3, panel b). In addition, treatment of RAW264.7 macrophages with several known endocytic

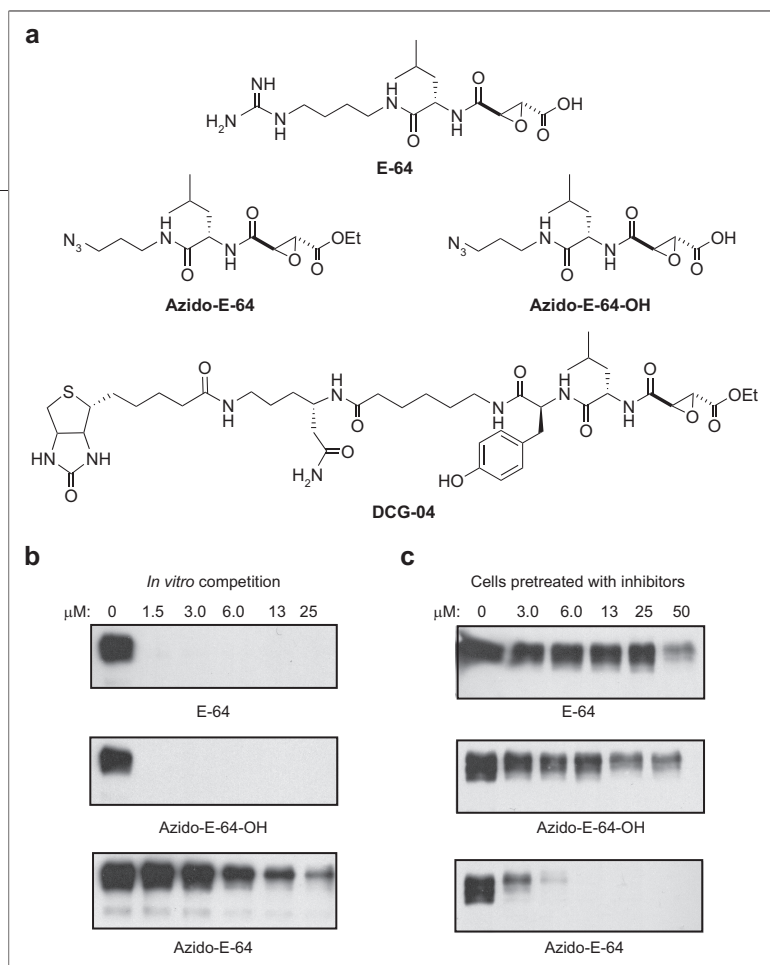


Figure 2. Azido-E-64 derivatives irreversibly inhibit Cat cysteine proteases *in vitro* and in cells. a) Mechanism-based irreversible inhibitors of Cat cysteine proteases based upon epoxysuccinate reactive group. b) Dose-dependent inhibition of DCG-04 labeling of RAW264.7 macrophage lysates treated with E-64, azido-E-64-OH, or azido-E-64. Cell lysates at pH 5.5 were labeled with DCG-04 (5 μ M) for 1 h in the presence of increasing concentrations of E-64, azido-E-64-OH, or azido-E-64. Reactions were terminated by acetone precipitation, and proteins were analyzed by streptavidin blotting. c) DCG-04 labeling of Cat cysteine proteases from RAW264.7 macrophages treated with E-64, azido-E-64-OH, or azido-E-64. Cells were incubated with increasing concentrations of E-64, azido-E-64-OH, or azido-E-64 for 1 h at 37 $^{\circ}$ C. Cell lysates at pH 5.5 were prepared and labeled with DCG-04 (5 μ M) for 1 h in the presence of increasing concentrations of E-64, azido-E-64-OH, or azido-E-64. Reactions were terminated by acetone precipitation, and proteins were analyzed by streptavidin blotting.

cysteine protease inhibitors prior to the addition of azido-E-64 inhibited the labeling of target proteins (Figure 3, panel c). Leupeptin, a broad-spectrum cysteine protease inhibitor, blocked the majority of azido-E-64 labeling, while the Cat B selective inhibitor (CA-074b-OMe) (27) primarily inhibited the labeling of a polypeptide at lower molecular weight (Figure 3, panel c), presumed to be Cat B (*vide infra*). Furthermore, addition of ammonium chloride or bafilomycin, a v-ATPase H^{+} pump inhibitor, both of which increase endosomal pH, also reduced azido-E-64 labeling (Figure 3, panel c). Conversely, the broad-spectrum aspartyl protease inhibitor pepstatin A had no effect on

azido-E-64 labeling (Figure 3, panel c). These data demonstrate that azido-E-64 targets active Cat cysteine proteases that function at low pH.

Azido-E-64 Selectively Targets Active Cat B in Macrophages. On the basis of the inhibitory activity of azido-E-64 measured by DCG-04 labeling (Figure 2), the molecular weight of the polypeptides labeled by azido-E-64, and their differential sensitivity to CA-074-OMe (Figure 3), the predominant protease targeted by azido-E-64 is most likely Cat B. To confirm that Cat B is indeed the most prominent target of azido-E-64, cell lysates from macrophages treated with or without azido-E-64 were labeled with p-biotin, incubated with streptavidin beads, and analyzed by streptavidin blot as well as by MS (Figures 1 and 4). As shown (Figure 4, panel a), Cat B was specifically recovered on streptavidin beads from azido-E-64 treated cell lysates following p-biotin labeling, as judged by anti-Cat B immunoblot. Moreover, polypeptides captured on streptavidin beads were denatured and then subjected to on-bead digestion with trypsin (Figure 1 and Figure 4, panel b). Tryptic peptides eluted from streptavidin beads were collected and sequenced by electrospray ionization (ESI) MS/MS. Comparison of peptides eluted from streptavidin beads revealed Cat B-specific peptides from azido-E-64 treated cell lysates, which were not present in control samples (Figure 4, panel b, and Supplementary Figure 2). To unequivocally establish Cat B as the major target for azido-E-64, bone marrow-derived macrophages (BMM ϕ s) prepared from wild-type and Cat B-deficient mice were labeled with azido-E-64. The major polypeptides specifically labeled by azido-E-64 in wild-type BMM ϕ s were identical in molecular weight compared to RAW264.7 macrophages (Figures 3 and 4). The major polypeptide labeled by azido-E-64 in wild-type BMM ϕ s is absent from Cat B-deficient BMM ϕ s. Importantly, the Cat B labeled by azido-E-64 in RAW macrophages and BMM ϕ s is the mature active enzyme (\sim 30 kDa), as no labeling of Cat B proform (\sim 39 kDa) was detected (Figures 3 and 4). We conclude that the primary target of azido-E-64 in macrophages is active Cat B.

Visualization of Active Cat B by Fluorescence Microscopy. Having established the specificity of azido-E-64 labeling for the active form of Cat B in macrophages, we investigated whether azido-E-64 labeling could be exploited for visualization of Cat B by fluorescence microscopy. BMM ϕ s were plated on cover-slips,

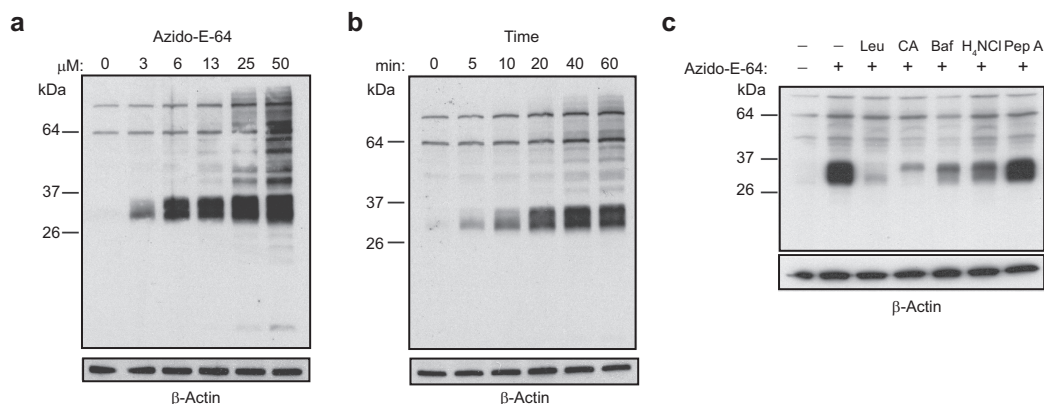


Figure 3. Visualization of Cat cysteine proteases labeled by azido-E-64 in living cells. **a)** Dose-dependent labeling of Cat cysteine proteases in RAW264.7 macrophages treated with azido-E-64. Cells were incubated with increasing concentrations of azido-E-64 for 1 h at 37 °C. Cells were harvested and lysed in the presence of protease inhibitor cocktail, and cell lysates were reacted with p-biotin (200 μ M) for 2 h at 37 °C. Reactions were terminated by acetone precipitation, and proteins were analyzed by streptavidin blotting. **b)** RAW264.7 macrophages were treated with azido-E-64 (20 μ M) for the time indicated. Visualization of azido-E-64 labeled proteins was performed as described above in panel a. **c)** RAW264.7 macrophages were treated with azido-E-64 (20 μ M) and lysosomal protease inhibitors Leupeptin (1 mM), CA-074-OMe (10 μ M), Bafilomycin (1 μ M), H₂NCl (50 mM), or Pepstatin A (10 μ M) for 1 h; harvested; and analyzed for azido-E-64 labeled proteins as described above in panel a.

treated with azido-E-64 or DMSO, fixed, and reacted *in situ* with p-biotin (Figures 1 and 5). The labeled cells were then stained with fluorescently conjugated streptavidin for imaging by spinning-disk confocal microscopy. To visualize endocytic compartments, BMM ϕ s were costained for lysosome-associated membrane glycoprotein 1 (LAMP-1) (Figure 5). Cells treated with azido-E-64 exhibited significant staining with fluorescent streptavidin compared to the DMSO control (Figure 5, top three panels), which demonstrates that azido-E-64 can be used to selectively visualize active Cat B in cells by fluorescence microscopy. The azido-E-64-specific staining resided within LAMP-1⁺ compartments, as expected for the labeling of endocytic proteases, and overlapped with Cat B protein that was visualized by anti-Cat B antibody staining (Figure 5). In contrast, azido-E-64 staining did not exhibit significant overlap with the distribution of protein disulfide isomerase (PDI), an endoplasmic reticulum (ER)-resident protein (Figure 5). These data demonstrate that azido-E-64 specifically labels Cat B in endocytic compartments where the active form of this protease is expected to reside. Similar results were also obtained with RAW264.7 macrophages (Supplementary Figure 3). We also analyzed monocyte-derived M ϕ s from class II MHC-eGFP knock-in mice (28) and observed spe-

cific azido-E-64 labeling that was blocked after pretreatment of cells with leupeptin or bafilomycin (Supplementary Figure 4). Collectively, these results establish that azido-E-64 labeling can be visualized not only by immunoblotting but also by fluorescence microscopy. The visualization of azido-E-64 labeling by fluorescence microscopy provides an additional measure of specificity as well as the means to monitor the activity of these proteases within subcellular compartments at the single-cell level.

Infection of Primary Macrophages with Live *Salmonella* Excludes Active Cat B from SCVs. The ability to specifically visualize active Cat cysteine proteases in living cells presented us with the unique opportunity to address the activity of these endocytic proteases during microbial infection of host cells. Intracellular bacterial pathogens have evolved sophisticated mechanisms to evade destruction by host cells to sustain a productive infection (29). *Salmonella* is an example of a facultative intracellular bacterial pathogen that exploits two type III secretion systems (TTSSs) to infect host cells and cause disease (29). These TTSSs form molecular syringes that inject protein substrates, termed “effectors”, into host cells to modulate cellular pathways for survival and replication (30). Upon invasion of host cells, *Salmonella* is

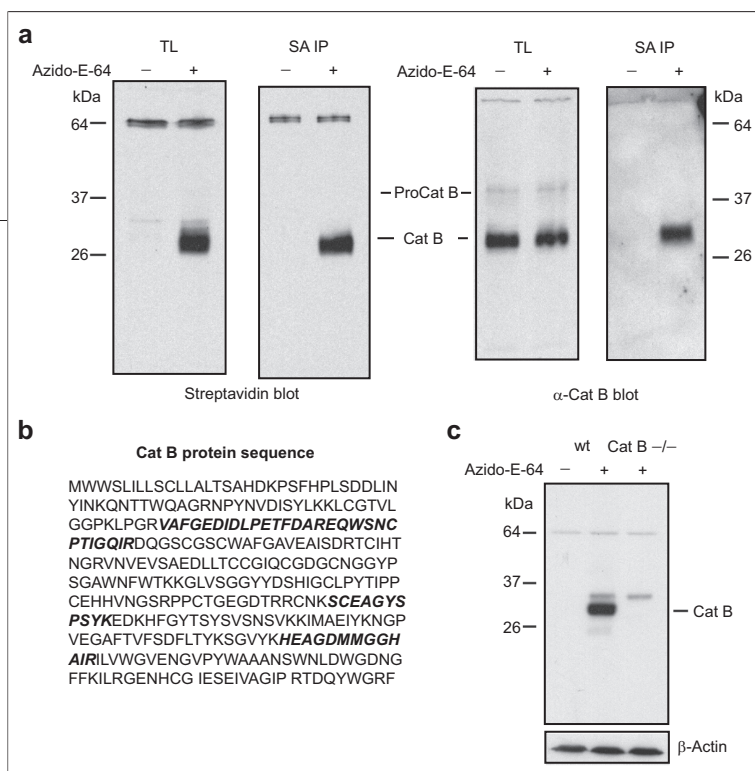


Figure 4. Azido-E-64 selectively labels Cat B in macrophages. **a)** Selective enrichment of Cat B from azido-E-64 treated macrophages after p-biotin labeling and incubation with streptavidin–agarose beads. TL = total lysate; SA IP = streptavidin–agarose immunoprecipitation **b)** Cat B protein sequence. Cat B peptides selectively identified from azido-E-64 treated samples after p-biotin labeling, streptavidin affinity enrichment, on-bead digestion, and MS sequencing are indicated in bold italic type. Cat B peptides recovered (MH⁺): **VAFGEDIDLPETFDAR** (1794.85), **EQWSNCPTIGQIR** (1588.78), **SCEAGYSPSYK** (1248.55), and **HEAGDMMGGHAIR** (1381.61). Representative MS/MS spectra of Cat B peptide is provided in Supplementary Figure 2. **c)** BMM ϕ s from wild-type and Cat B $-/-$ mice were treated with DMSO (–) or 20 μ M azido-E-64 (+). Streptavidin-HRP blots were inactivated with H₂O₂ and probed with anti- β -actin antibody to demonstrate equal levels of protein loading.

thought to inhibit phago-lysosome fusion and resides in an SCV, a unique endocytic compartment (31). The SCV is devoid of oxidative burst enzymes, such as NADPH oxidase (32) and inducible nitric oxide synthase (33) that enable the bacteria to avoid degradation by reactive radical species. Endocytic compartments are also rich in degradative enzymes that include the Cat family of aspartyl, cysteine, and serine proteases, which have been implicated in antigen processing and presentation (34), but their roles in *Salmonella* infection remain unclear.

The Cat families of proteases are synthesized as zymogens that are processed into their mature, active forms upon arrival in endocytic compartments. Here their activities are controlled by subcellular localization, the presence of endogenous inhibitors or activators, and pH (35). Reports that document the association of these endocytic proteases with *Salmonella* in host cells yield a mixed outcome (36). In epithelial cell lines infected with *S. typhimurium*, Cat D does not exhibit significant overlap with SCVs at early time points of infection as

assessed by immunocytochemistry but appears to be recruited at late stages of infection during *Salmonella*-induced filament formation (37–39). Cat D and L were also absent from SCVs in macrophage-like cell lines and were not recruited over the course of the infection (40, 41). In contrast, SCVs in primary BMM ϕ s were shown to associate with Cat L over the course of the *Salmonella* infection (42). Furthermore, sucrose-gradient purification of SCVs from a macrophage cell line recovered proforms of Cat D and L, as demonstrated by immunoblot analysis (43, 44), which suggests that *Salmonella* may reside in an endocytic compartment with inactive proteases. However, the recovery of calnexin, an ER-resident protein, from purified SCVs suggests that proforms of endocytic proteases may be recruited to SCVs prior to their arrival into endocytic compartments (44), possibly through an ER-phagosome fusion pathway (45, 46). While it is clear that avirulent or heat-killed bacteria are targeted to lysosomes for degradation, reports on the interactions between endocytic proteases and live *Salmonella* present conflicting conclusions, particularly the studies that pertain to macrophages. Because the activities of these endocytic proteases are controlled post-translationally, it is imperative to assess whether the proteases associated with intracellular bacteria are indeed enzymatically active.

To determine whether active endocytic proteases are present in SCVs of primary macrophages, we assayed azido-E-64 labeling of active Cat B in *Salmonella*-infected BMM ϕ s. BMM ϕ s plated on cover glass slips were infected with *S. typhimurium* at a multiplicity of infection (MOI) of \sim 100 for 1 h and labeled with azido-E-64 for 30 min. Following fixation of *S. typhimurium*-infected BMM ϕ s, azide-modified polypeptides were reacted with p-biotin and prepared for fluorescence microscopy. Azido-E-64 efficiently labeled LAMP-1⁺ compartments of *Salmonella*-infected BMM ϕ s, but azido-E-64 labeling was completely absent from SCVs as judged by costaining with anti-*Salmonella* antibody (Figure 6). The lack of azido-E-64 labeling in SCVs was reproducible over several independent infections of BMM ϕ s, where multiple *Salmonella*-infected macrophages were analyzed. Furthermore, the segregation of active Cat B from SCVs, as assessed by azido-E-64 labeling, was not a transient phenomenon and persisted over 4 h postinfection (data not shown). The azido-E-64 labeling was also specific for Cat B, as no detectable azido-E-64 labeling was observed in Cat B-deficient BMM ϕ s

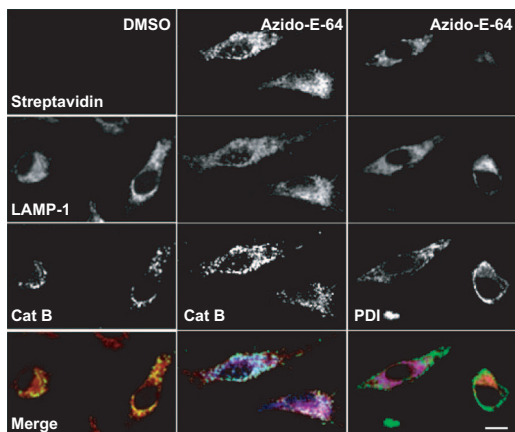


Figure 5. Immunofluorescence analysis of active Cat B in BMMø cells labeled with azido-E-64. BMMø cells were treated with DMSO or azido-E-64 (20 μ M), fixed, reacted with p-biotin, and stained with AlexaFluor647-conjugated streptavidin. LAMP-1 was visualized by staining with rat anti-mouse LAMP-1 followed by AlexaFluor595-conjugated anti-rat. Cat B or PDI was visualized by staining with rabbit polyclonal sera for Cat B and PDI, respectively, followed by AlexaFluor488-conjugated anti-rabbit. Images were acquired by spinning-disk confocal microscopy. For merged images, AlexaFluor647-conjugated streptavidin (blue) and LAMP-1 (red), Cat B (green), or PDI (green). Scale bar represents 10 μ m.

infected with *S. typhimurium* (Figure 6). Most bacteria were degraded when heat-killed *Salmonella* were used to infect BMMø cells, but the bacteria that remained inside LAMP-1⁺ compartments of macrophages colocalized with active Cat B, which demonstrates the exclusion of active Cat B from SCVs required live *Salmonella* (Figure 6).

Exclusion of Active Cat B from Bacteria-Containing Vacuoles Is Specific to Salmonella. To determine whether the exclusion of active Cat B from bacteria-containing vacuoles in BMMø cells was specific for *S. typhimurium* or simply a general property of intracellular bacteria, we generated monomeric-red fluorescent protein (mRFP)-labeled *S. typhimurium* and nonpathogenic *Escherichia coli* and compared their localization within BMMø cells with that of active Cat B, as judged by azido-E-64 labeling. SCVs in BMMø cells infected with mRFP *S. typhimurium* were also devoid of active Cat B (Figure 7), which is consistent with our results using anti-*Salmonella* polyclonal sera (Figure 6). In contrast, internalized mRFP *E. coli* targeted to LAMP-1⁺ compartments were mostly

degraded and colocalized with active Cat B (Figure 7). Together, these observations suggest that the exclusion of active Cat B from bacteria-containing vacuoles in BMMø cells is specific to live *Salmonella* and not a general property exhibited by bacteria inside host cells (Figure 7).

The development of mechanism-based probes has yielded new chemical tools for dissecting the function of protein superfamilies in biology not accessible by genomics and proteomics (1). Neither transcriptional profiling nor immunocytochemical detection of the polypeptides can uncover regulatory non-template-encoded phenomena, such as ionic environment, or the presence of modulators of enzyme activity, either endogenous or specified by pathogens. These probes have enabled the profiling of enzyme activities in complex mixtures for several enzyme families and identified new enzymatic activities not predicted by bioinformatics (1). While it is clear that mechanism-based probes are making a contribution to biology, the application of mechanism-based probes to living cells is still challenging. Here we demonstrate that a single-mechanism-based probe, azido-E-64, not only can be used to visualize Cat B in living cells but also allows affinity enrichment for MS-based proteomic analysis with phosphine reagents via the Staudinger ligation (Figure 1).

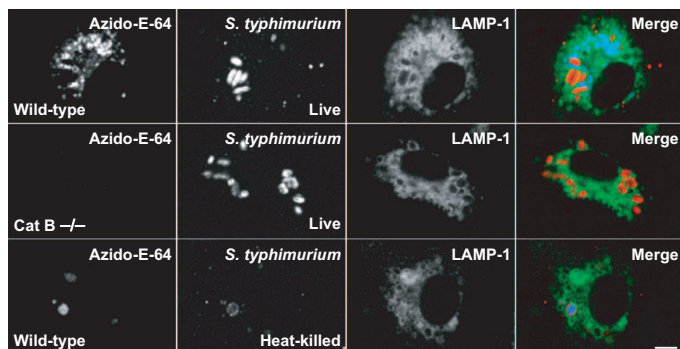


Figure 6. Visualization of active Cat B in *S. typhimurium*-infected BMMø cells. BMMø cells were infected with live or heat-killed *S. typhimurium* (MOI = 100) for 1 h, washed and labeled with azido-E-64 (20 μ M), and visualized as described in Figure 6. *S. typhimurium* rabbit was visualized by staining with anti-*S. typhimurium* polyclonal sera, followed by AlexaFluor568-conjugated anti-rabbit. LAMP-1 was visualized by staining with rat anti-mouse LAMP-1 followed by AlexaFluor488-conjugated anti-rat. Images were acquired by spinning-disk confocal microscopy. For merged images, AlexaFluor647-conjugated streptavidin (blue), *S. typhimurium* (red), and LAMP-1 (green). Scale bar represents 5 μ m.

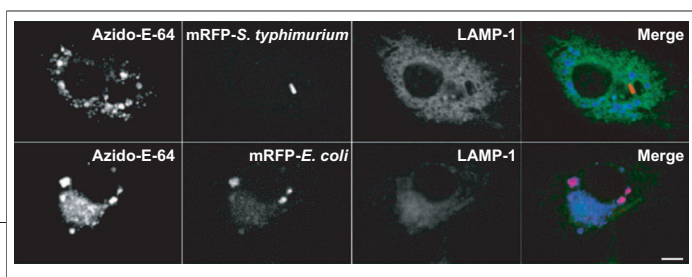


Figure 7. The exclusion of active Cat B from bacteria-containing vacuoles is specific to *S. typhimurium*-infected BMM ϕ s. BMM ϕ s were infected with mRFP *S. typhimurium* or mRFP *E. coli* (MOI = 100) for 1 h, washed and labeled with azido-E-64 (20 μ M), and visualized as described in Figure 6. LAMP-1 was visualized by staining with rat anti-mouse LAMP-1 followed by AlexaFluor488-conjugated anti-rat. Images were acquired by spinning-disk confocal microscopy. For merged images, AlexaFluor647-conjugated streptavidin (blue), mRFP *S. typhimurium* and mRFP *E. coli* (red), and LAMP-1 (green). Scale bar represents 5 μ m.

Many pathogens infect host cells through endocytic pathways to co-opt host nutrient and biosynthetic machinery for survival and replication (29). Within the endocytic compartment of host cells, pathogens face a broad arsenal of host factors and enzymes that are capable of destroying them. As a consequence, many successful intracellular pathogens have evolved sophisticated mechanisms to evade destruction. The interactions between pathogens and host cells are very complex and require new tools to dissect mechanisms of immune evasion. Cell-permeable mechanism-based probes provide new opportunities to investigate host-pathogen interactions not possible with genomics or proteomics. *Salmonella* in particular traffics into a unique endocytic compartment, the *Salmonella*-containing vacuole, which allows the bacterium to survive and replicate in epithelial cells and macrophages. Unlike *Mycobacterium tuberculosis*, which inhibits vacuole acidification (47), *Salmonella* actively decreases endosomal pH (~4.0–6.0) to enhance intracellular survival (48), conditions that are compatible with the pH optima of endocytic proteases (35). The Cat cysteine proteases are the most abundant proteolytic enzymes in endocytic compartments and are involved in many biological processes, ranging from bone resorption, tumor metastasis, antigen presentation, and viral infection, as well as transcription regulation or apoptosis (49). While a few studies suggest that these endocytic proteases are excluded (40, 41) or differentially processed (43, 44) in SCVs of macrophage-like cell lines, Cat cysteine proteases do associate with SCVs of primary macrophages (42). As a result, the activity of Cat cysteine proteases during bacterial infections is unclear.

To monitor the activities of the Cat cysteine proteases during *Salmonella* infection, we utilized azido-E-64 to visualize Cat B in macrophages after bacterial infection. Following infection of BMM ϕ s with *Salmonella*, labeling with azido-E-64 showed that active Cat B was absent from SCVs at early time points of infection, a trait that persisted for several hours after internalization of bacte-

ria. The exclusion of active Cat B from bacteria-containing vacuoles was specific to live *Salmonella*, as the distribution of heat-killed *Salmonella* or *E. coli* within BMM ϕ s completely overlapped with azido-E-64 labeling. These data are consistent with previous immunofluorescence studies that show Cat D and L polypeptides to be absent from SCVs in macrophage cell lines (40, 41). Moreover, the lack of azido-E-64 labeling within SCVs of primary BMM ϕ s is in agreement with the association of SCVs with inactive proforms of endocytic proteases recovered by sucrose-gradient purification (43, 44). These studies suggest *Salmonella* may encode specific gene products, possibly secreted into SCVs that inhibit endocytic protease activity or interfere with the conversion of inactive proteases into their mature active enzymes. In addition to modification of phago-lysosome fusion (50), *Salmonella* may also interfere with endocytic protease activity directly to survive and replicate inside macrophages. Future studies with *Salmonella* mutants should enable the dissection of specific genes that are responsible for the exclusion or inhibition of active endocytic proteases from SCVs.

In conclusion, the two-step labeling approach reported here provides a nonradioactive method to evaluate the activity of the Cat cysteine proteases in living cells and also allows affinity enrichment of labeled proteins for MS-based proteomic analysis. In addition, the ability to perform fluorescence microscopy with mechanism-based probes allows the visualization of enzyme activities within subcellular compartments of individual cells, the biochemical evaluation of which is often problematic because the organelles concerned are often difficult to obtain in pure form, particularly for complex series of events such as infection with a pathogen. Thus, the application of this chemical approach to other intracellular pathogens that reside in endocytic compartments should provide further insight into the mechanisms by which these pathogens manage to evade degradation by host cells. The extension of this approach to other mechanism-based probes should broaden their utility for studies in living cells and animal models. Collectively, cell-permeable mechanism-based probes should provide a powerful means to measure changes in enzyme activity *in vivo* and afford the possibility of examining biological activities that are controlled post-translationally.

METHODS

Cell Culture. RAW264.7 macrophages were cultured in DMEM supplemented with 10% fetal calf serum (FCS), 100 units mL⁻¹ penicillin, and 0.1 mg mL⁻¹ streptomycin, and cells were incubated in a 5% CO₂ humidified incubator at 37 °C. Bone marrow cells were harvested by flushing the femur and tibia of wild-type C57BL/6 mice using a 25-gauge needle. For BMMø, 2 × 10⁶ bone marrow cells were plated on 100 × 20 mm tissue culture plates in complete DMEM media supplemented with 10% FCS, 100 units mL⁻¹ penicillin, 0.1 mg mL⁻¹ streptomycin, and macrophage-colony stimulating factor derived from the supernatant of L929 cells. Fresh media was replenished on days 4 and 7.

Treatment of Mø with Inhibitors. Mø were seeded ~2.0 × 10⁶ cells per well in six-well polystyrene tissue culture plates with 1 mL of media. Cells were then supplemented with protease inhibitors (E-64 or azido-E-64) by adding the appropriate volume from 10 mM DMSO stock solutions. After incubation of cells for 37 °C for the times indicated, cells were washed twice with phosphate-buffered saline (PBS) and harvested.

DCG-04 Labeling of Cell Lysates. Cell pellets from ~2.0 × 10⁶ cells were resuspended in 100 µL of ice-cold pH 5.5 lysis buffer (0.1% Triton x-100, 0.5% CHAPS, 50 mM citrate, 5 mM dithiothreitol (DTT), pH 5.5) and centrifuged at 4 °C for 10 min at 20,000g. The supernatant (cell lysate) was collected, and the protein concentration was determined by Bradford assay (BioRad). Cell lysates (50 µg) were reacted with 5 µM of DCG-04 with or without (E-64 or azido-E-64) for 2 h at 37 °C in a final reaction volume of 50 µL. The reactions were terminated by addition of ice-cold acetone, incubated at -20 °C for 20 min, and centrifuged at 4 °C for 10 min at 20,000g to precipitate proteins. The supernatant was discarded, and the protein pellet was resuspended in SDS-protein loading buffer with 2-mercaptoethanol.

P-Biotin Labeling of Cell Lysates. Cell pellets from ~2.0 × 10⁶ cells were resuspended in 100 µL of ice-cold NP-40 lysis buffer (0.5% NP-40, 50 mM Tris, 5 mM MgCl₂, pH 7.4) with Complete Mini protease inhibitor cocktail and centrifuged at 4 °C for 10 min at 20,000g. The supernatant (cell lysate) was collected, and the protein concentration was determined by Bradford assay (BioRad). Staudinger ligation labeling of azide-modified proteins was performed by incubation of cell lysates (50 µg) with 250 µM p-biotin (5 mM in DMSO stock) and 5 mM DTT in total reaction volume of 50 µL for 2 h at 37 °C. The reactions were terminated by addition of ice-cold acetone (1 mL), and the product was incubated at -20 °C for 20 min and centrifuged at 4 °C for 10 min at 20,000g to precipitate proteins. The supernatant was decanted, and the protein pellet was resuspended in SDS-protein loading buffer with 2-mercaptoethanol.

Immunoblotting. P-biotin (~20 µg) and DCG-04 (~10 µg) labeled proteins were separated by SDS-PAGE (12.5% gel) and transferred to a polyvinylidene fluoride membrane, and the membrane was blocked with 5% nonfat dried milk in PBS/Tween 20 (PBST) (PBS, 0.1% Tween 20, pH 7.4) overnight at 4 °C or 1 h at RT. The membrane was washed with PBST (3 × 10 mL) and incubated with streptavidin-HRP (1:5000 in PBST) for 1 h, washed with PBST (3 × 25 mL), and developed using Western Lighting Chemiluminescence Reagent Plus (Perkin Elmer). To demonstrate equal levels of protein loading, streptavidin-HRP blots were inactivated with H₂O₂ and probed with anti-β-actin antibody followed by rabbit anti-mouse HRP. Anti-Cat B immunoblots were performed with rabbit anti-Cat B polyclonal and then probed with mouse anti-rabbit HRP.

Streptavidin Affinity Enrichment and Proteomic Analysis of Biotinylated Proteins. Cell lysates (5 mg) from macrophages treated with or without azido-E-64 were reacted with 25 µM p-biotin (5 mM in DMSO stock) and 5 mM DTT in a total reaction volume of 5 mL for 2 h at 37 °C with rocking. The reactions were

terminated by addition of ice-cold acetone (40 mL), and the resulting product was incubated at -20 °C for 20 min and centrifuged at 4 °C for 10 min at 4000g to precipitate proteins. The supernatant was decanted, and the protein pellet was resuspended in 5 mL of 0.2% SDS (50 mM Tris, pH 7.4) with sonication. Proteins were precipitated again with ice-cold acetone (40 mL) and resuspended in 5 mL of 0.2% SDS (50 mM Tris, pH 7.4) with sonication to remove any residue p-biotin. Pre-washed streptavidin-agarose beads (250 µL) were then added to protein lysates (1 mg mL⁻¹) and allowed to incubate at 4 °C for 1 h with rocking. Streptavidin-agarose beads were centrifuged for 5 min at 4000g at 4 °C and washed with 10 mL of 0.2% SDS (50 mM Tris, pH 7.4) four times. One-fifth of the streptavidin-agarose beads (~50 µL of slurry) were removed, resuspended in SDS-protein loading buffer with 2-mercaptoethanol, and analyzed by immunoblotting as described above. The remaining streptavidin-agarose beads (~200 µL) were washed with 1 mL of 50 mM NH₄CO₃, pH 7.4, twice, denatured, and reduced with 500 µL of 6 M urea, 10 mM tris(2-carboxyethyl)phosphine, 50 mM NH₄CO₃, pH 7.4, for 30 min at RT with rocking. Iodoacetamide from a stock solution of 1 M was added to streptavidin-agarose beads to give a final concentration of 20 mM iodoacetamide and allowed to react for 30 min at RT with rocking in the dark. The beads were then washed with 1 mL of 50 mM NH₄CO₃, pH 7.4, three times, resuspended in 500 µL of 50 mM NH₄CO₃, pH 7.4, with 2 µg of porcine trypsin, and allowed to digest overnight at 37 °C with rocking. The streptavidin beads were centrifuged for 1 min at 4000g, and the supernatants were collected and concentrated by SpeedVac. Recovered peptides were analyzed by reverse-phase LC ESI-MS using Waters nanoAquity-UPLC coupled to a Thermo LTQ linear ion-trap mass spectrometer. MS/MS spectra were searched by SEQUEST against the NCBI database (nr.fasta.hr 6/27/2006). SEQUEST results were analyzed with Bioworks Browser 3.2 and filtered with the following criteria: different peptides; minimum cross correlation coefficients (1, 2, 3 charge states) of 1.50, 2.00, 2.50; number different peptides of 2 per protein and Sp preliminary score of 500.

Fluorescence Microscopy. Mø (~2.0 × 10⁵ per well) were seeded in an eight-well chambered Lab-Tek II cover glass slides 16 h before analysis. Mø on cover glass slides were treated with DMSO or 20 µM azido-E-64 in 250 µL of media for 30 min at 37 °C, washed with PBS, and fixed with ice-cold methanol for 5 min at 4 °C. After fixation, cells were washed with PBS and reacted with 250 µM p-biotin in 200 µL of PBS for 2 h at 37 °C. The cells were then washed with PBS and blocked with 10% bovine serum albumin (BSA) in PBS for 16 h at 4 °C or 1 h at RT. The cells were stained with primary antibodies dissolved in permeabilization buffer (10% BSA, 0.5% saponin in PBS) for 1 h at RT, washed with permeabilization buffer (3 × 250 µL), and stained with fluorescently conjugated secondary antibodies or streptavidin dissolved in permeabilization buffer for 1 h at RT in the dark. Slides were washed with permeabilization buffer (2 × 250 µL), PBS, and samples were mounted with Fluoromount G (Southern Biotech) and analyzed using a Perkin-Elmer spinning disk confocal microscope with UltraView software.

Bacterial Infection of BMMø. BMMø (~2.0 × 10⁵ per well) were seeded in eight-well chambered Lab-Tek II cover glass slides the 16 h before analysis and infected with bacteria (MOI = ~100), centrifuged at 500g for 5 min, and incubated for 1 h at 37 °C. The cells were washed with PBS (250 µL × 2) and labeled with 20 µM azido-E-64 for 20 min at 37 °C. BMMø were fixed and stained for immunofluorescence and analyzed as described above.

Acknowledgments: H.C.H. acknowledges the Damon Runyon Cancer Research Foundation for a postdoctoral fellowship. J.L. thanks the Gulbenkian Ph.D. Program in Biomedicine and the Portuguese Science and Technology Foundation for a predoctoral fel-

lowship. A.W.M.v.d.W. acknowledges Philip Morris USA, Inc., for support. R.M. was supported by a Boehringer Ingelheim Fonds predoctoral fellowship. A.M.P. acknowledges the National Science Foundation for a graduate fellowship. Y.-M.K. acknowledges the Leukemia and Lymphoma Society for a postdoctoral fellowship. This work was funded by NIH Grants to M.N.S. (AI055962) and H.L.P. (5RO1A1034893-13).

Supporting Information Available: This material is available free of charge via the Internet.

REFERENCES

- Evans, M. J., and Cravatt, B. F. (2006) Mechanism-based profiling of enzyme families, *Chem. Rev.* **106**, 3279–3301.
- Liu, Y., Patricelli, M. P., and Cravatt, B. F. (1999) Activity-based protein profiling: the serine hydrolases, *Proc. Natl. Acad. Sci. U.S.A.* **96**, 14694–14699.
- Borodovsky, A., Ovaa, H., Kolli, N., Gan-Erdene, T., Wilkinson, K. D., Ploegh, H. L., and Kessler, B. M. (2002) Chemistry-based functional proteomics reveals novel members of the deubiquitinating enzyme family, *Chem. Biol.* **9**, 1149–1159.
- Greenbaum, D., Medzihradszky, K. F., Burlingame, A., and Bogoy, M. (2000) Epoxide electrophiles as activity-dependent cysteine protease profiling and discovery tools, *Chem. Biol.* **7**, 569–581.
- Kato, D., Boatright, K. M., Berger, A. B., Nazif, T., Blum, G., Ryan, C., Chehade, K. A., Salvesen, G. S., and Bogoy, M. (2005) Activity-based probes that target diverse cysteine protease families, *Nat. Chem. Biol.* **1**, 33–38.
- Chan, E. W., Chattopadhyaya, S., Panicker, R. C., Huang, X., and Yao, S. Q. (2004) Developing photoactive affinity probes for proteomic profiling: hydroxamate-based probes for metalloproteases, *J. Am. Chem. Soc.* **126**, 14435–14446.
- Saghatelian, A., Jessani, N., Joseph, A., Humphrey, M., and Cravatt, B. F. (2004) Activity-based probes for the proteomic profiling of metalloproteases, *Proc. Natl. Acad. Sci. U.S.A.* **101**, 10000–10005.
- Raskin, D. M., Seshadri, R., Pukatzki, S. U., and Mekalanos, J. J. (2006) Bacterial genomics and pathogen evolution, *Cell* **124**, 703–714.
- Greenbaum, D. C., Baruch, A., Grainger, M., Bozdech, Z., Medzihradszky, K. F., Engel, J., DeRisi, J., Holder, A. A., and Bogoy, M. (2002) A role for the protease falcipain 1 in host cell invasion by the human malaria parasite, *Science* **298**, 2002–2006.
- Kattenhorn, L. M., Korbel, G. A., Kessler, B. M., Spooner, E., and Ploegh, H. L. (2005) A deubiquitinating enzyme encoded by HSV-1 belongs to a family of cysteine proteases that is conserved across the family *Herpesviridae*, *Mol. Cell* **19**, 547–557.
- Schlieker, C., Korbel, G. A., Kattenhorn, L. M., and Ploegh, H. L. (2005) A deubiquitinating activity is conserved in the large tegument protein of the *Herpesviridae*, *J. Virol.* **79**, 15582–15585.
- Misaghi, S., Balsara, Z. B., Catic, A., Spooner, E., Ploegh, H. L., and Stambach, M. N. (2006) Chlamydia trachomatis-derived deubiquitinating enzymes in mammalian cells during infection, *Mol. Microbiol.* **61**, 142–150.
- Artavanis-Tsakonas, K., Misaghi, S., Comeaux, C. A., Catic, A., Spooner, E., Duraisingh, M. T., and Ploegh, H. L. (2006) Identification by functional proteomics of a deubiquitinating/deNeddylating enzyme in *Plasmodium falciparum*, *Mol. Microbiol.*, in press.
- Lennon-Dumenil, A. M., Bakker, A. H., Maehr, R., Fiebiger, E., Overkleeft, H. S., Roseblatt, M., Ploegh, H. L., and Lagaudriere-Gesbert, C. (2002) Analysis of protease activity in live antigen-presenting cells shows regulation of the phagosomal proteolytic contents during dendritic cell activation, *J. Exp. Med.* **196**, 529–540.
- Greenbaum, D., Baruch, A., Hayrapetian, L., Darula, Z., Burlingame, A., Medzihradszky, K. F., and Bogoy, M. (2002) Chemical approaches for functionally probing the proteome, *Mol. Cell. Proteomics* **1**, 60–68.
- Joyce, J. A., Baruch, A., Chehade, K., Meyer-Morse, N., Giraudo, E., Tsai, F. Y., Greenbaum, D. C., Hager, J. H., Bogoy, M., and Hanahan, D. (2004) Cathepsin cysteine proteases are effectors of invasive growth and angiogenesis during multistage tumorigenesis, *Cancer Cell* **5**, 443–453.
- Blum, G., Mullins, S. R., Keren, K., Fonovic, M., Jedeszko, C., Rice, M. J., Sloane, B. F., and Bogoy, M. (2005) Dynamic imaging of protease activity with fluorescently quenched activity-based probes, *Nat. Chem. Biol.* **1**, 203–209.
- Saxon, E., and Bertozzi, C. R. (2000) Cell surface engineering by a modified Staudinger reaction, *Science* **287**, 2007–2010.
- Wang, Q., Chan, T. R., Hilgraf, R., Fokin, V. V., Sharpless, K. B., and Finn, M. G. (2003) Bioconjugation by copper(I)-catalyzed azide-alkyne [3 + 2] cycloaddition, *J. Am. Chem. Soc.* **125**, 3192–3193.
- Speers, A. E., Adam, G. C., and Cravatt, B. F. (2003) Activity-based protein profiling, *in vivo* using a copper(I)-catalyzed azide-alkyne [3 + 2] cycloaddition, *J. Am. Chem. Soc.* **125**, 4686–4687.
- Ovaa, H., Van Swieten, P. F., Kessler, B. M., Leeuwenburgh, M. A., Fiebiger, E., Van Den Nieuwendijk, A. M., Galardy, P. J., Van Der Marel, G. A., Ploegh, H. L., and Overkleeft, H. S. (2003) Chemistry in living cells: detection of active proteasomes by a two-step labeling strategy, *Angew. Chem., Int. Ed.* **42**, 3626–3629.
- Sprung, R., Nandi, A., Chen, Y., Kim, S. C., Barma, D., Falck, J. R., and Zhao, Y. (2005) Tagging-via-substrate strategy for probing O-GlcNAc modified proteins, *J. Proteome Res.* **4**, 950–957.
- Sieber, S. A., Niessen, S., Hoover, H. S., and Cravatt, B. F. (2006) Proteomic profiling of metalloprotease activities with cocktails of active-site probes, *Nat. Chem. Biol.* **2**, 274–281.
- Speers, A. E., and Cravatt, B. F. (2005) A tandem orthogonal proteolysis strategy for high-content chemical proteomics, *J. Am. Chem. Soc.* **127**, 10018–10019.
- Hanada, K., Tamai, M., Yamaguchi, M., Ohmura, S., Sawada, J., and Tanaka, I. (1978) Isolation and characterization of E-64, a new thiol protease inhibitor, *Agric. Biol. Chem.* **42**, 523–528.
- Powers, J. C., Asgian, J. L., Ekici, O. D., and James, K. E. (2002) Irreversible inhibitors of serine, cysteine, and threonine proteases, *Chem. Rev.* **102**, 4639–4750.
- Buttle, D. J., Murata, M., Knight, C. G., and Barrett, A. J. (1992) CA074 methyl ester: a proinhibitor for intracellular cathepsin B, *Arch. Biochem. Biophys.* **299**, 377–380.
- Boes, M., Cerny, J., Massol, R., Op den Brouw, M., Kirchhausen, T., Chen, J., and Ploegh, H. L. (2002) T-cell engagement of dendritic cells rapidly rearranges MHC class II transport, *Nature* **418**, 983–988.
- Monack, D. M., Mueller, A., and Falkow, S. (2004) Persistent bacterial infections: the interface of the pathogen and the host immune system, *Nat. Rev. Microbiol.* **2**, 747–765.
- Galan, J. E. (2001) *Salmonella* interactions with host cells: type III secretion at work, *Annu. Rev. Cell Dev. Biol.* **17**, 53–86.
- Brumell, J. H., and Grinstein, S. (2004) *Salmonella* redirects phagosomal maturation, *Curr. Opin. Microbiol.* **7**, 78–84.
- Vazquez-Torres, A., Xu, Y., Jones-Carson, J., Holden, D. W., Lucia, S. M., Dinauer, M. C., Mastroeni, P., and Fang, F. C. (2000) *Salmonella* pathogenicity island 2-dependent evasion of the phagocyte NADPH oxidase, *Science* **287**, 1655–1658.
- Chakravorty, D., Hansen-Wester, I., and Hensel, M. (2002) *Salmonella* pathogenicity island 2 mediates protection of intracellular *Salmonella* from reactive nitrogen intermediates, *J. Exp. Med.* **195**, 1155–1166.
- Honey, K., and Rudensky, A. Y. (2003) Lysosomal cysteine proteases regulate antigen presentation, *Nat. Rev. Immunol.* **3**, 472–482.
- Turk, V., Turk, B., and Turk, D. (2001) Lysosomal cysteine proteases: facts and opportunities, *EMBO J.* **20**, 4629–4633.
- Holden, D. W. (2002) Trafficking of the *Salmonella* vacuole in macrophages, *Traffic* **3**, 161–169.

37. Brumell, J. H., Tang, P., Mills, S. D., and Finlay, B. B. (2001) Characterization of *Salmonella*-induced filaments (Sifs) reveals a delayed interaction between *Salmonella*-containing vacuoles and late endocytic compartments, *Traffic* 2, 643–653.
38. Garcia-del Portillo, F., and Finlay, B. B. (1995) Targeting of *Salmonella typhimurium* to vesicles containing lysosomal membrane glycoproteins bypasses compartments with mannose 6-phosphate receptors, *J. Cell Biol.* 129, 81–97.
39. Meresse, S., Steele-Mortimer, O., Finlay, B. B., and Gorvel, J. P. (1999) The rab7 GTPase controls the maturation of *Salmonella typhimurium*-containing vacuoles in HeLa cells, *EMBO J.* 18, 4394–4403.
40. Garvis, S. G., Beuzon, C. R., and Holden, D. W. (2001) A role for the PhoP/Q regulon in inhibition of fusion between lysosomes and *Salmonella*-containing vacuoles in macrophages, *Cell. Microbiol.* 3, 731–744.
41. Rathman, M., Barker, L. P., and Falkow, S. (1997) The unique trafficking pattern of *Salmonella typhimurium*-containing phagosomes in murine macrophages is independent of the mechanism of bacterial entry, *Infect. Immun.* 65, 1475–1485.
42. Oh, Y. K., Alpuche-Aranda, C., Berthiaume, E., Jinks, T., Miller, S. I., and Swanson, J. A. (1996) Rapid and complete fusion of macrophage lysosomes with phagosomes containing *Salmonella typhimurium*, *Infect. Immun.* 64, 3877–3883.
43. Hashim, S., Mukherjee, K., Raj, M., Basu, S. K., and Mukhopadhyay, A. (2000) Live *Salmonella* modulate expression of Rab proteins to persist in a specialized compartment and escape transport to lysosomes, *J. Biol. Chem.* 275, 16281–16288.
44. Mills, S. D., and Finlay, B. B. (1998) Isolation and characterization of *Salmonella typhimurium* and *Yersinia pseudotuberculosis*-containing phagosomes from infected mouse macrophages: *Y. pseudotuberculosis* traffics to terminal lysosomes where they are degraded, *Eur. J. Cell Biol.* 77, 35–47.
45. Jutras, I., and Desjardins, M. (2005) Phagocytosis: at the crossroads of innate and adaptive immunity, *Annu. Rev. Cell Dev. Biol.* 21, 511–527.
46. Touret, N., Paroutis, P., and Grinstein, S. (2005) The nature of the phagosomal membrane: endoplasmic reticulum versus plasma-membrane, *J. Leukocyte Biol.* 77, 878–885.
47. Sturgill-Koszycki, S., Schlesinger, P. H., Chakraborty, P., Haddix, P. L., Collins, H. L., Fok, A. K., Allen, R. D., Gluck, S. L., Heuser, J., and Russell, D. G. (1994) Lack of acidification in *Mycobacterium phagosomes* produced by exclusion of the vesicular proton-ATPase, *Science* 263, 678–681.
48. Coombes, B. K., Brown, N. F., Valdez, Y., Brumell, J. H., and Finlay, B. B. (2004) Expression and secretion of *Salmonella* pathogenicity island-2 virulence genes in response to acidification exhibit differential requirements of a functional type III secretion apparatus and SsaL, *J. Biol. Chem.* 279, 49804–49815.
49. Lecaille, F., Kaleta, J., and Bromme, D. (2002) Human and parasitic papain-like cysteine proteases: their role in physiology and pathology and recent developments in inhibitor design, *Chem. Rev.* 102, 4459–4488.
50. Buchmeier, N. A., and Heffron, F. (1991) Inhibition of macrophage phagosome-lysosome fusion by *Salmonella typhimurium*, *Infect. Immun.* 59, 2232–2238.